

# Calorimetric evolution of the early pozzolanic reaction of natural zeolites

R. Snellings · G. Mertens · J. Elsen

Received: 24 June 2009 / Accepted: 27 August 2009 / Published online: 10 September 2009  
© Akadémiai Kiadó, Budapest, Hungary 2009

**Abstract** The pozzolanic reaction between natural zeolite tuffs, portlandite and water was investigated over the course of the early reaction period up to 3 days. Isothermal conduction calorimetry experiments supplemented by TG/DTG and XRD analyses assisted in the elucidation of the sequence of reaction processes taking place. The calorimetry experiments clearly showed the dependence of the pozzolanic reaction rate and associated heat release on the fineness of the zeolite tuff. Higher external surface areas of pozzolans yield higher total heat releases. Also the exchangeable cation content of the zeolites influences the reaction rate. Release of exchangeable alkalis into solution promotes the pozzolanic reaction by raising the pH and zeolite solubility. The appearance of an exotherm after approximately 3 h of reaction is more conspicuous when alkali-rich zeolites are reacted. This exotherm is conceived to be related to a transformation or rupture of initially formed reaction products covering the zeolite grains. The formation of substantial amounts of ‘stable’ calcium silicate hydrate (C–S–H) and calcium aluminate hydrate (C–A–H) reaction took place after an induction period of more than 6 h. The openness of the zeolite framework affects the proneness of the zeolite to dissolution and thus its reactivity. Open framework zeolites such as chabazite were observed to react much more rapidly than closed framework zeolites such as analcime.

**Keywords** Pozzolanic reaction · Zeolites · Lime · Conduction calorimetry

## Introduction

Addition of supplementary cementitious materials or pozzolans to Portland cement offers the advantages of a lowered economical and environmental unit cost of the resulting blended cement. Pozzolans are materials that combine with portlandite ( $\text{Ca}(\text{OH})_2$ ) or portlandite releasing materials in the presence of water to form reaction products with binder properties [1]. Hydrated blended cements are also more durable due to the consumption of the excess portlandite levels liberated during the cement hydration process. Moreover, the formation of additional binding calcium–silicate–hydrate (C–S–H; cement chemistry notation:  $C = \text{CaO}$ ,  $S = \text{SiO}_2$ ,  $H = \text{H}_2\text{O}$ ,  $A = \text{Al}_2\text{O}_3$ ,  $\check{C} = \text{CO}_2$ , the hyphenation indicates a variable stoichiometry) reaction products in the pozzolanic reaction lowers the cement permeability. Consequently, cement susceptibility to corrosion and other deleterious reactions is decreased [2].

A promising group of pozzolanic materials is natural zeolite tuffs formed in the alteration process of vitric pyroclastic deposits. Earlier research showed that natural zeolite tuffs are more reactive than their unaltered counterparts and many artificial pozzolans such as blast furnace slag and fly ash [3–6]. Natural zeolite tuffs are frequently used on a empirical basis as a pozzolanic additive in regions where deposits are readily available (e.g., Italy, Greece, Turkey and China).

The zeolite content of the tuff, the particle size distribution and the external specific surface were found to exert an important influence on the early pozzolanic reactivity [7]. Furthermore, the zeolite structure and crystal chemistry were observed to play a prominent role. The release of exchangeable cations, especially alkalis, changed the solution chemistry, the reaction kinetics on the short term

R. Snellings (✉) · G. Mertens · J. Elsen  
Department of Earth and Environmental Sciences, KU Leuven,  
Celestijnenlaan 200E, Box 2410, 3001 Heverlee, Belgium  
e-mail: ruben.snellings@ees.kuleuven.be

and the reaction product assemblage [7–9]. The zeolite structure and framework Si/Al ratio affected mainly the progress of reaction at later ages. Open framework zeolites with a high silica content showed a higher long-term pozzolanic reactivity [7]. However, the underlying reactions and role of the zeolite crystal structure and chemistry on the pozzolan reactivity remain largely unresolved, especially during the early hours and days of the reaction.

This article reports on the calorimetry of the early pozzolanic reaction between portlandite and various natural zeolite tuffs up to 3 days of reaction. Isothermal conduction calorimetry experiments were performed to investigate the nature and sequence of chemical exothermal reactions which occur after the mixing of natural zeolite tuffs, portlandite and water. A simultaneous evaluation of the reaction progress and formation of reaction products by thermogravimetry (TG) and X-ray powder diffraction (XRD) contributed to the elucidation of the reaction mechanism.

## Materials and methods

The pozzolan activity of seven zeolite tuffs was investigated. Tuffs predominantly composed of one zeolitic phase, namely analcime, chabazite, clinoptilolite, erionite or phillipsite were selected (Table 1). Commercial hydrated lime, containing portlandite and a minor amount of calcium carbonate, was obtained from Lhoist S.A. Elkem microsilica 983U was used as a reference pozzolanic material. The origin of the zeolite tuff samples is reported in Table 1. Conjointly, the results of a chemical and physical characterization are given. Bulk chemical composition was determined by X-ray Fluorescence (XRF) spectroscopy and Loss On Ignition (LOI). Semi-quantitative microanalyses of the zeolite crystal chemistry were performed on a Scanning Electron Microscope (SEM) equipped with an Energy Dispersive X-ray analyser (EDX) system. The particle size distributions of the ground zeolite materials were analysed by laser-diffractometry, the external surface area of the materials was determined by t-plots of the N<sub>2</sub> adsorption isotherms using the Harkins–Jura thickness model in the range 0.60–0.90 nm. A quantitative assessment of the phase composition of the tuffs was performed by the Rietveld refinement of X-ray powder diffraction patterns, the results are presented in Table 2. For detailed accounts of the experimental procedures for the chemical, physical and mineralogical characterization of the sample materials the reader is referred to Mertens et al. [7].

All samples were wet milled with hexane in a McCrone Micronising Mill® to reduce particle size dimensions to similar mean diameter ( $d_{50}$ ) values of 5–10 µm for all

zeolite tuffs. To evaluate the effect of particle size diameter on the pozzolanic reactivity Cli2 clinoptilolite tuff was ground to coarse (C), fine (F) and very fine (VF) particle size distributions (cf. Table 1). To assess the influence of exchangeable cation content on the reaction thermochemistry, Cli3 clinoptilolite tuff was exchanged in nearly saturated Na-, K-, and Ca-acetate solutions at 60 °C.

The prepared zeolite samples were mixed with portlandite in a 1:1 ratio and thoroughly blended. Isothermal conduction calorimetry measurements were performed on a TA Instruments TAM Air device. Approximately, 4 g of the reactant powders were blended with equal amounts of distilled water and introduced into sealed calorimeter flasks. Subsequently, the flasks were placed in the calorimeter and data were recorded during isothermal reaction at 20 °C. All reactants were equilibrated to room temperature prior to the experiment.

A duplicate set of reactant powders was mixed with water in a 1:1 proportion, transferred to sealed poly-ethylene containers and stored at 20 °C in a thermostatically controlled room. At 6 h, 1 day and 3 days of reaction the hydrated pastes were vacuum-dried in order to halt the hydration reaction by removing evaporable water. The resulting powders were analysed by TG and XRD to follow the reaction progress. TG measurements were done on a Netzsch STA 409 PC Luxx®, the samples were heated at 10 °C/min in a continuous N<sub>2</sub> flow. The residual contents of portlandite were determined from TG following the method of Taylor [10], in which the calculated portlandite content is corrected for the continuous dehydration of other components over the portlandite decomposition interval. The amount of portlandite consumed over time is conveniently taken as the degree of reaction or the reactivity of a specific pozzolanic material [11–13].

The formation of crystalline reaction products was followed by XRD. The equipment used was a Phillips PW1830 device with CuK $\alpha_{1,2}$  radiation at 30 mA and 45 kV using a graphite monochromator and a gas proportional detector. Data were collected in Bragg–Brentano geometry from 5 to 70° 2 $\theta$ , with a step size of 0.02° 2 $\theta$  and 2 s counting time per step.

## Results

### Isothermal conduction calorimetry

The patterns of the rate of heat release and cumulative evolved heat for the Cli2 sample ground to varying particle size distributions are given in Fig. 1. Directly after the blending of the powders with water a strong peak in heat evolution rate was reached in all pastes. The initial heat release subsided gradually during the first hours of

**Table 1** Characteristics, sample origin, chemical composition and physical properties of the zeolite tuffs

Sample name	Main mineral	Sample origin	Chemistry							SEM-EDX	t-plot	External surface area/m <sup>2</sup> g <sup>-1</sup>	d <sub>50</sub> /μm	Grain Size			
			SiO <sub>2</sub>	Al <sub>2</sub> O <sub>3</sub>	Na <sub>2</sub> O	CaO	K <sub>2</sub> O	TiO <sub>2</sub>	Fe <sub>2</sub> O <sub>3</sub>	LOI	SUM	Bulk atomic Si/Al	Atomic Si/Al zeolites				
Ana	Analcime	Unknown	62.90	15.81	8.82	0.63	1.10	0.17	0.10	1.26	7.67	98.46	3.5	2.6	4.5	9.35	
Phi	Phillipsite	Naples (Italy)	54.43	16.00	2.71	2.39	7.67	0.21	0.39	3.15	11.28	98.23	3.0	2.8	12.9	6.29	
Cha	Chabazite	Christmas Arizona (USA)	52.11	13.45	3.47	2.03	1.42	0.46	0.31	1.91	20.12	95.28	3.4	3.2	34.9	5.17	
Eri	Eronite	Pine Valley Nevada (USA)	57.90	13.64	5.36	0.39	3.47	0.15	0.06	1.15	16.54	98.66	3.7	3.7	9.0	4.86	
Cli1	Clinoptilolite	Cayo Formation (Ecuador)	58.48	15.52	0.96	3.71	2.07	0.32	0.46	2.24	15.85	96.60	4.1	4.6	17.0	8.20	
Cli2	Clinoptilolite	Simav Graben (Turkey)	62.09	12.35	1.18	1.88	4.17	0.21	0.21	1.15	14.02	97.26	4.4	4.7	18.5	3.97	
Cli2_VF															14.7	8.45	
Cli2_F																	
Cli2_C																	
Cli_3	Clinoptilolite	Zlatokop (Serbia)	64.14	11.26	1.01	3.37	1.01	0.22	0.16	0.97	14.49	96.62	5.0	4.6	22.7	4.9	20.97
Cli3_Na																	
Cli3_Ca																	
Cli3_K																	
SF	Silica Fume	Elkem Micro-silica 983U	98.25	0.29	0.07	0.19	0.20	0.02	0.00	0.04	0.75	99.81	±300	n/a	10.1	0.2	

**Table 2** Quantitative phase content (wt%) of the selected zeolite tuffs

Sample	Ana	Phi	Cha	Eri	Cli_1	Cli_2	Cli_3
Analcime	73.3	7.6					
Phillipsite		31.6					
Chabazite		9.4	67.6	6.4			
Erionite				90.0			
Clinoptilolite					98.9	84.5	83.8
Quartz	16.4		2.4	0.7	1.1	0.7	3.8
Cristobalite						1.5	
Plagioclase	0.7		1.7				6.5
Anorthoclase		14.2	3.1	2.2		5.5	
K-feldspar	7.4	29.0				4.2	
Augite		3.7					0.4
Muscovite 2M1			5.6		3.6		2.6
Calcite	0.9						2.8
Gypsum				1.1			
Sum	98.6	95.5	80.4	100.4	100.1	99.9	99.9
Unidentified	1.4	4.5	19.6				

Main zeolite components are in italics

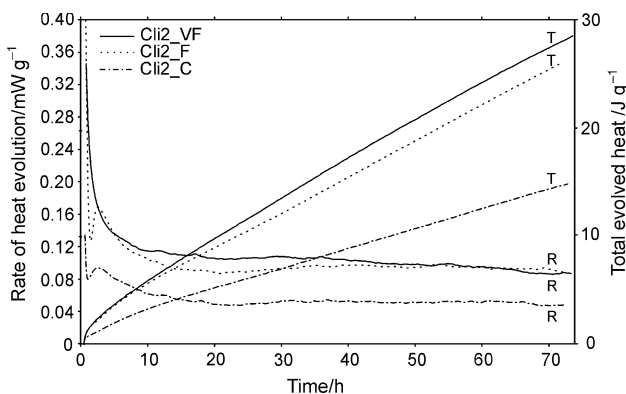


**Fig. 1** Rate of heat evolution R and total evolved heat T of reacting Cli2\_VF, Cli2\_F and Cli2\_C portlandite pastes

reaction. The decrease in the rate of heat release and the eventually attained level in rate of heat evolution were dependent on the fineness of the zeolite tuff in the paste. The finest clinoptilolite material, Cli2\_VF, showed a longer continuation of the initial exotherm and higher rates of heat evolution ensuing the initial peak than their coarser ground counterparts. However, in contrast to the coarser samples, the finest materials did not show a second superimposed peak at approximately 3 h of reaction. The latter peak is characterized by a relatively rapid increase in rate of heat evolution followed by a slower decrease, resulting in an asymmetric peak shape. Subsequently, rates of heat evolution remained approximately constant over the 3 days time interval. The cumulative sums of the heat released showed that the total evolved heat is obviously dependent on the particle size distribution.

A comparison of the rate of heat evolution and total released heat during the pozzolanic reaction of the selected zeolite tuff materials and the microsilica reference is given in Fig. 2. After the initial peak in Fig. 2a, a second conspicuous peak at approximately 2.5–3 h of reaction can be recognized for the Cha, Eri, Cli1, Cli3 and Phi samples, no second peak was found for the Ana sample. The SF reference showed only a slight shoulder. Furthermore, large differences were encountered in the rate of heat evolution in the subsequent period up to 72 days. The Cha and SF pastes continuously showed the highest heat release and an additional third broad peak was identified. Heat release was significantly lower for the other pastes, especially for the Ana paste. The presence of a third broad peak was less obvious. The rates of heat evolution in the latter samples remained relatively constant or showed only a minor increase.

The calorimetry measurements for the cation exchanged Cli3 samples are depicted in Fig. 3. When compared to the other portlandite–zeolite pastes, it is apparent that the tail of the initial peak is in all cases broad. In fact, at the time when a second peak already occurred for the other pastes, the tails of the initial peaks were still dominating the rate of heat release curves for the exchanged samples. The subsequent level of heat evolution rate is relatively high. The Cli3\_K paste showed a lower and constant rate of heat release than the Cli3\_Na and Cli3\_Ca pastes. A broad peak similar to the third peak in the Cha and SF paste can be

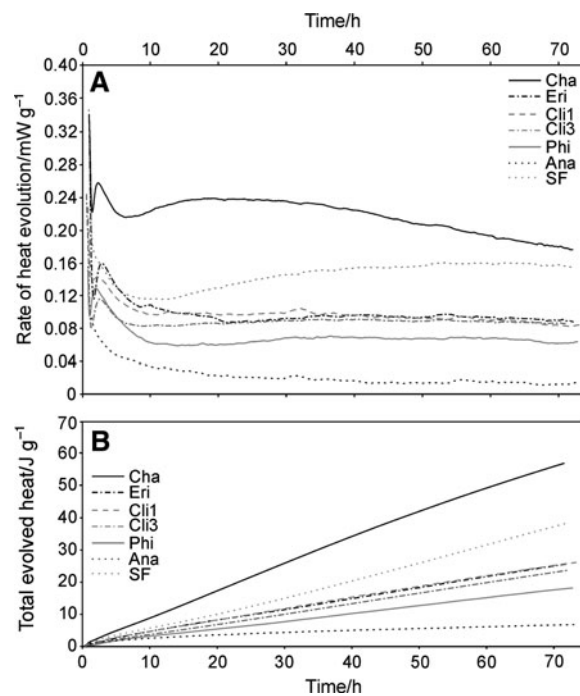


**Fig. 2** Rate of heat evolution (a) and total evolved heat (b) of the reacting pastes of portlandite and selected tuffs containing different types of naturally occurring zeolites

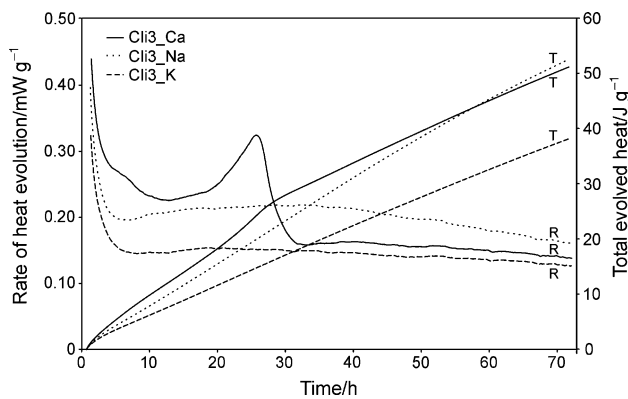


**Fig. 3** Rate of heat evolution R and total evolved heat T of reacting pastes of portlandite and Cli3 exchanged to Ca, Na and K

recognized for the Na-exchanged clinoptilolite tuff. In contrast, the Ca-exchanged clinoptilolite tuff presented a very different behaviour. After the initial burst of heat, a slight shoulder, similar but later than in the SF paste, appeared. However, the Cli3\_Ca deviated mostly in the appearance of a marked peak in the rate of heat release at approximately 25 h of reaction and a rapid decrease to an approximately constant value afterwards.

#### Thermogravimetry and X-ray diffraction

To relate the sequence of calorimetric events to the consumption of starting materials and formation of reaction products, the calorimetric curves were compared with TG and XRD data at specific time intervals of 6, 24 and 72 h of reaction. The consumption of portlandite, determined by TG, is generally considered to indicate the reactivity of the pozzolanic material. The residual portlandite content of the pastes through time is given in Table 3. The lowered levels of portlandite calculated from TG at 6 h with respect to the initial proportion in the sample are due to the uptake of significant amounts of non-evaporable water. Comparing Table 3 with Fig. 2 it can be deduced that pastes which released larger amounts of heat effectively consumed more portlandite over the 6 h to 3 days period. The concerned zeolite tuffs can thus be regarded as more reactive.

Figures 4 and 5 show XRD and DTG data for the reacted portlandite–Cha and portlandite–Cli3\_Ca pastes,

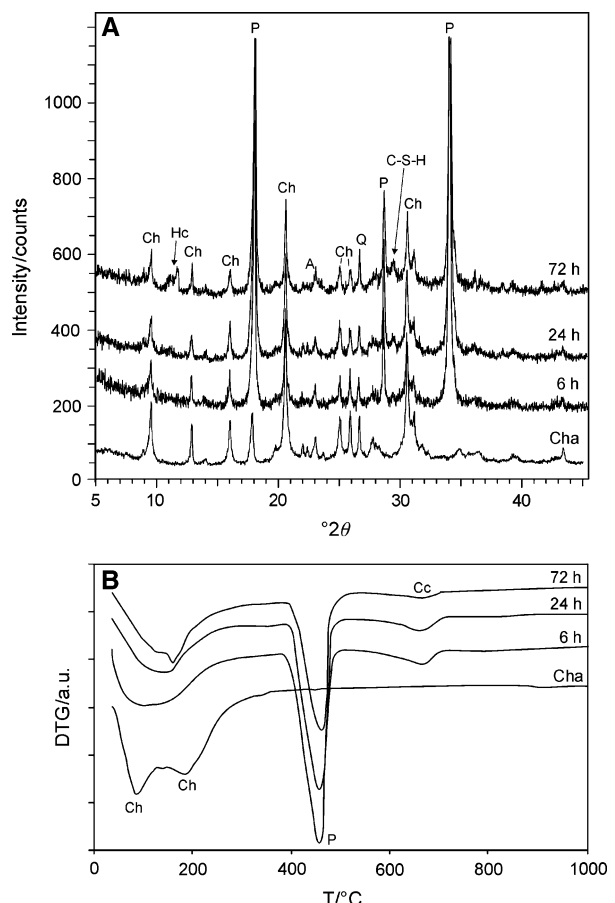


**Fig. 4** **a** XRD patterns of pure Cha and reacted portlandite–Cha paste at 6, 24 and 72 h of reaction. Ch identifies with chabazite, Hc with hydrocalumite, P with portlandite, A with anorthoclase, Q with quartz and C–S–H with C–S–H. **b** DTG curves of pure Cha and the reacted portlandite–Cha pastes

respectively. The development of reaction products followed a similar pattern in all pastes, Figs. 4 and 5 are therefore representative. At 6 h of reactions negligible amounts of reaction products were identified in the TG and XRD patterns. The dehydration peak in the 60–200 °C range can be attributed largely to the loss of zeolite water. After 1 day of reaction additional peaks of the reaction products are observed, which become more pronounced after 3 days of reaction. The encountered reaction products are calcium aluminate hydrates and calcium silicate

**Table 3** Residual amount of unreacted portlandite determined by TG

Time (h)	Portlandite content/wt%												
	Ana	Phi	Cha	Eri	Cli1	Cli2_VF	Cli2_F	Cli2_C	Cli3	Cli3_Na	Cli3_Ca	Cli3_K	SF
6	41.5	39.6	37.2	39.0	39.6	40.6	40.8	41.9	38.4	38.4	41.3	40.9	34.6
24	41.4	39.2	34.5	38.7	37.9	38.1	39.0	40.2	35.5	35.5	39.5	35.2	35.0
72	40.6	34.6	26.9	33.6	33.4	33.2	35.2	36.7	31.0	27.1	33.4	30.9	30.5

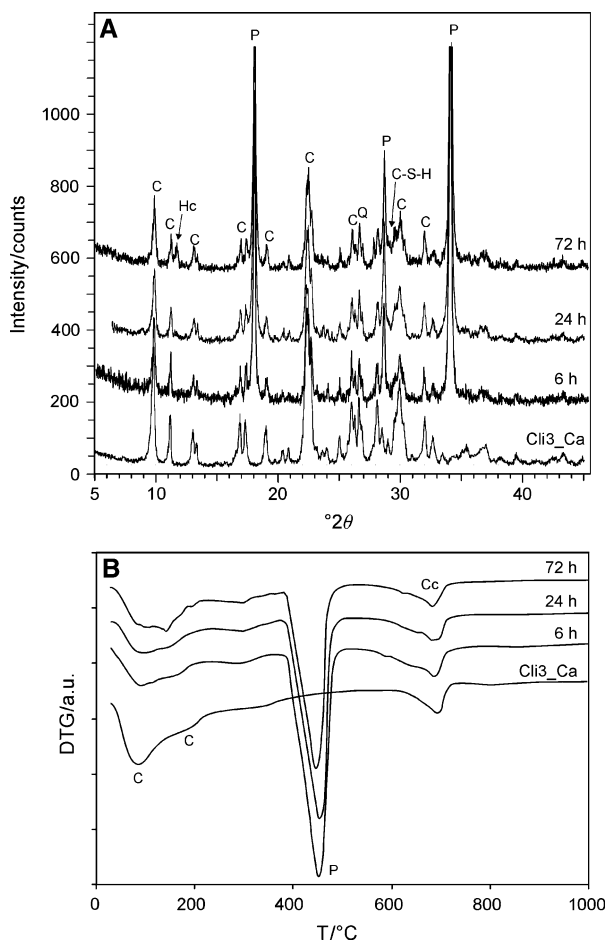


**Fig. 5** **a** XRD patterns of pure  $\text{Cli}_3\text{Ca}$  and reacted portlandite- $\text{Cli}_3\text{Ca}$  paste at 6, 24 and 72 h of reaction. C stands for clinoptilolite, Hc for hydrocalumite, P for portlandite, Q for quartz and C–S–H for C–S–H. **b** DTG curves of pure  $\text{Cli}_3\text{Ca}$  and the reacted portlandite- $\text{Cli}_3\text{Ca}$  pastes

hydrates. The calcium aluminate hydrates could be identified as hexagonal calcium aluminate hydrates or hydrocalumite containing carbonate in the interlayers ( $\text{C}_4\text{A}\dot{\text{C}}\text{H}_{11}$ ), with a *d*-spacing of 7.6 Å in the XRD patterns and a superimposed negative peak in the DTG pattern at approximately 150 °C [10]. Hydrocalumite typically forms as a product of the pozzolanic reaction of aluminosilicates and portlandite [1, 3]. Hexagonal calcium aluminate hydrates are very prone to carbonation by air or by contact with calcium carbonate impurities in the portlandite. The weakly crystalline C–S–H phase can be identified by the intensity rise of the diffuse main peak around 3.06 Å *d*-spacing. The C–S–H phase typically displays a broad main peak of dehydration around 120 °C [10].

The start of reaction product formation after the initial 6-h period confirms earlier findings that the actual pozzolanic reaction involving zeolites at 20 °C initiates after 6 h [8]. The relationship of the amount of portlandite consumed and reaction products formed with the total heat evolved at 72 h

suggests that the third broad peak in the calorimetry measurements can be attributed to the pozzolanic reaction and the formation of hydrated reaction products.

## Discussion

### Reaction mechanism

Calorimetric measurements are frequently used in the elucidation of the reaction sequence in the hydration of cements or cement components such as  $\text{C}_3\text{S}$  (elite) [1, 10, 14, 15] or in hydrated mixtures of reactive pozzolans such as metakaolin and portlandite or cement [16–20]. The isothermal calorimetry patterns of the early portlandite–zeolite pozzolanic reaction reveal several consecutive exotherms which can be related to a sequence of exothermal reactions broadly similar to earlier reported accounts of the pozzolan–portlandite reaction.

Initially, a first intense peak occurred upon mixing of the portlandite–zeolite powders with water, this peak was not completely resolved due to mixing outside the calorimeter cell. Several processes are reported to occur upon wetting the sample. First of all, adsorption processes release enthalpy. Water is adsorbed on the particle surfaces, and especially for zeolites a significant amount of water can be absorbed within the porous framework. It was shown that initial water adsorption in zeolite–lime systems occurs very rapidly and involves changes in unit-cell parameters and volume. This is interpreted as the exothermal relaxation of the zeolite structure in an aqueous medium [8, 21]. The exothermal dissolution of portlandite ( $\text{Ca}(\text{OH})_2$ ) in the aqueous medium occurs rapidly and a pH of 12.7 or higher is reached [1, 14]. In response  $\text{Si}-\text{OH}$ , and  $\text{Al}-\text{OH}$  groups on the zeolite surface are dissociated to  $\text{Si}-\text{O}^-$  and  $\text{Al}-\text{O}^-$  and  $\text{Ca}^{2+}$  cations from the portlandite-saturated solution are adsorbed on the surface [1, 15]. The formation of  $\text{Si}-\text{O}^-$  and  $\text{Al}-\text{O}^-$  bonds weakens connected  $\text{Si}-\text{O}$  and  $\text{Al}-\text{O}$  bonds in the lattice of the surface (Gutmann rules [21]) and facilitates the detachment of silicate and aluminate tetrahedra [22]. The dissolution rate is proportional to the surface concentration of  $\text{Si}-\text{O}^-$  and  $\text{Al}-\text{O}^-$  or the pH [23]. The negative zeolite framework charge renders diffusion of negatively charged hydroxyls into the zeolite pore network energetically highly unfavourable. In consequence, the authors consider the initial zeolite framework dissolution process as essentially a surface-driven process which is consequently related to the external specific surface of the zeolite materials. This is corroborated by a more intense and enduring heat release from the finely and very finely ground zeolite tuffs in Fig. 1. The release and exchange of channels cations are known to be faster and independent from the dissolution of framework ions [23].

After reaching a critical solubility product the dissolved aluminate and silicate species recombine and precipitate with  $\text{Ca}^{2+}$  to form a layer of initial products covering the zeolite particles [1, 15, 24]. The formation of a similar initial reaction product layer is generally conceived to cause the decrease in heat release and reaction rate after the initial peak in cement hydration [15]. The subsequent appearance of a second, minor exothermal peak or shoulder around 3 h of reaction has also been observed in the pozzolanic reaction of SF and metakaolin with portlandite [11, 16–18]. This feature was explained in various ways, i.e., the formation of C–S–H and C–A–H reaction products [14, 16], the increased dissolution rate of solid species into the alkaline solution [17] or the combination of surface silanol groups with  $\text{Ca}^{2+}$  [18]. Here, the amount of reaction products formed after the second exotherm is negligible as exemplified in Figs. 4 and 5, contradicting the former explanation for this system. Furthermore, the asymmetric peak shape suggests a sudden appearance and acceleration of the occurring process, contradicting both latter explanations which are not considered to be self-reinforcing due to the resulting formation of a covering layer of products. More interesting is the mechanism proposed by Double et al. [25] for the hydration of  $\text{C}_3\text{S}$  and adapted for the pozzolanic reaction by Takemoto and Uchikawa [1]. The initially formed surface layer of products after the first exotherm would grow and become semi-permeable. Alkali cations released from the dissolving zeolites would be contained within the enveloping reaction product layer and a concentration gradient would build up over the layer. Inward diffusion of water by osmotic pressure would disintend the layer and eventually lead to the disruption of the boundary layer [1]. The release of dissolved species and precipitation of products would result in an abrupt increase in the enthalpy released. Interesting to note is that especially pozzolans containing large amount of alkalis would display a similar behaviour [1]. This complies with the observation in Fig. 2 that in the zeolite–portlandite reaction especially zeolites rich in easily exchangeable alkalis showed a pronounced second peak in the rate of heat release. Additionally, the asymmetric peak shape can be explained by the waning of the reaction after the rupture of the enveloping C–S–H boundary layer.

More recent models for the hydration of  $\text{C}_3\text{S}$  propose that the dissolution of the initially formed ‘unstable’ C–S–H and nucleation of a ‘stable’ C–S–H phase causes the beginning of the setting process in cement [15]. In this view, transformation of the C–S–H boundary layer from a gel type phase to more crystalline products could also cause the liberation of the enclosed dissolved species.

The continuous rate of heat evolution or the appearance of a third broad peak can be related to the continuous pozzolanic reaction as evidenced by the formation of C–S–H

and  $\text{C}_4\text{A}\overset{\circ}{\text{C}}\text{H}_{11}$  reaction products by TG and XRD (Figs. 4, 5). This complies with earlier studies [8] in that the formation of significant amounts of reaction products occurs after a so-called induction period.

### Pozzolanic reactivity

When comparing the consumption of portlandite and the heat evolution curves of  $\text{Cl}_1\text{I}_2$  ground to different grain sizes it is apparent that the mean grain size diameter and the related external surface area influenced both the early heat evolution and the rate of heat release during the pozzolanic reaction. More portlandite was consumed in the finer mixtures. This can obviously explain the relation between the concentration of surface sites or available external surface and the reaction rate. The absence of a clearly resolved second peak in the portlandite– $\text{Cl}_1\text{I}_2$ \_VF paste can possibly be explained by the overlap with the extended first exotherm.

The dependence of the pozzolan reactivity on the type of exchangeable cations was described earlier based on extensive TG and XRD experiments [7, 8]. Based on the amount of reacted portlandite, Na- and K-exchanged clinoptilolites showed a higher reactivity than Ca-exchanged clinoptilolite. This is explained by the rise in pH and simultaneous increase in silicate solubility caused by the exchange of alkalis with  $\text{Ca}^{2+}$  in solution.  $\text{K}^+$  is less easily exchanged than  $\text{Na}^+$ . In consequence, the early reactivity was lower for K-exchanged samples. In contrast, Ca-exchanged clinoptilolite would hamper portlandite consumption by the additional  $\text{Ca}^{2+}$  delivered to the solution. The pozzolan reactivity based on the TG results can be similarly interpreted, however, the peculiar rate of heat evolution behaviour observed in Fig. 3 for the Ca-exchanged sample remains difficult to explain. The relatively high heat evolution occurring around 26 h of reaction cannot be related to the formation of crystalline reaction products other than those forming in the alkali-exchanged clinoptilolite–portlandite pastes as differing products were not observed by TG nor XRD. The higher hydration enthalpy of the  $\text{Ca}^{2+}$  cation compared to  $\text{Na}^+$  and  $\text{K}^+$  could partially account for the higher rate of heat evolution displayed during the first day. It is also plausible that the changed solution chemistry modifies the type of initial C–S–H formed, especially the evolution of C/S ratio would be different. Snellings et al. [8] have shown that the structure of the C–S–H phase in similar reacted portlandite–Ca-exchanged clinoptilolite pastes tended to evolve differently than the C–S–H phase formed by the pozzolanic reaction with alkali-exchanged clinoptilolites. The evolution of the latter was indicative for the formation of longer silicate chains and lower C/S ratio. The presence of substantial concentrations of  $\text{Ca}^{2+}$  and silica near the pozzolan

surface could have resulted in the formation of more ill-crystalline C–S–H at early reaction times. This C–S–H formation could accelerate when crystals grow larger and subsequently slow down when diffusion control becomes the rate-determining process.

The correlation between available surface area and pozzolan reactivity demonstrated for Cli2 is considerably worsened when all tested materials are taken into account. This indicates that individual sample characteristics such as phase composition and chemistry additionally control the amount of lime consumed. The sample mineralogy is dominated by (alumino-)silicates, more specifically naturally occurring zeolites. Disregarding the exchangeable cation content, zeolite stability can be generally correlated with the Si/Al ratio and the framework packing density [26]. The first factor depends on the lower bonding energy of Al[4]-O compared to Si[4]-O, more Al-rich pozzolans could thus be expected to react more rapidly. This reasoning was shown to be inconsistent with the pozzolan reactivity of the analcime tuff. Though analcime contained a large amount of tetrahedrally coordinated Al, the residual amount of unreacted lime was high. Similarly, Mertens et al. [7] observed that high silica zeolites showed higher degrees of reaction over longer periods of reaction up to 6 months. The lower analcime reactivity can be accounted for by the low external specific surface and the higher packing density. In contrast, the slightly more siliceous chabazite tuff showed an elevated early reactivity, even surpassing the reactivity of silica fume. The main difference with Ana is situated in the open zeolite framework geometry of chabazite, facilitating cation exchange and framework dissolution. Furthermore, the external surface area of Cha is much higher. The differences in available external surface area for reaction seem to correlate well with the observed variations in the amount of portlandite consumed by the Cli1, Cli2 and Cli3 samples ground to similar grain sizes. In parallel with the observations for the variously ground Cli2 sample, the appearance of the second superimposed exotherm is better resolved in the Cli1 and Cli2 samples with lower external surface areas. It should be mentioned that also differences in the exchangeable cation content of the clinoptilolites could play a role.

An additional factor is the amount of reactive aluminosilicate compounds present in the zeolite materials. Though phillipsite has a relatively low framework density and the Phi sample contained additional chabazite and analcime, the overall zeolite content was low compared to other samples, resulting in a lower reactivity than expected based upon the available external surface area and the zeolite stability. Alkali feldspars (anorthoclase and K-feldspar) present in large amounts are conceived to be much more stable than zeolites due to their dense framework structure [26] and thus less reactive.

## Conclusions

The rate of heat release curves typically showed an intense exotherm immediately after mixing the zeolite–portlandite powders with water. Contributing exothermal processes are water adsorption on zeolite surfaces and within zeolite, hydration and solvation of exchanged and dissolved metal cations. Dissolution of portlandite initiates surface controlled hydrolysis of the zeolite and precipitation of C–S–H gel on the zeolite surface. The transformation or rupture of this first cover of reaction products due to the changing solution environment can explain the occurrence of a second exothermal peak after approximately 3 h of reaction. This peak is better resolved in mixtures containing reactive alkali-rich zeolites. The ensuing formation of ‘stable’ C–S–H and  $C_4A\dot{C}H_{11}$  reaction products resulting from the recombination of silica and alumina from the zeolite and Ca from portlandite is identified as a broad exotherm or an elevated continuous level of heat release.

The dependence of the early pozzolan reactivity on the zeolite tuff fineness and external surface area strongly suggests that the pozzolanic reaction is a surface driven process.

The zeolite exchangeable cation content exerts an important influence on the solution chemistry, especially the pH of the solution is raised when alkalis are exchanged for  $Ca^{2+}$  in solution. The rising pH effectuates an increased silicate solubility and changes the structural evolution of the main C–S–H reaction product. The deviating thermal behaviour of the Ca-exchanged clinoptilolite from that of the alkali-exchanged clinoptilolites in the pozzolanic reaction likely originates from the differing solution chemistry.

Open framework aluminosilicates such as chabazite are much more prone to dissolution than closed framework structures such as analcime or feldspars. Finally, it is obvious that the overall reactive zeolite content of zeolite tuff is an important control on the overall pozzolanic reactivity of the material.

**Acknowledgements** The authors would like to thank L. Machiels, J. Minet, E. Passaglia, V. Simic and P. Verlooy for the contribution of sample material. The experimental assistance of O. Cizer was appreciated. An anonymous reviewer is gratefully acknowledged for the constructive comments. The first two authors are aspirants of the Research Foundation - Flanders (FWO).

## References

1. Takemoto K, Uchikawa T. Hydratation des ciments pouzzolaniques. Proceedings of the 7th international congress on the chemistry of cement, vol IV-2. Paris; 1980. p. 1–29.
2. Janotka I, Krajci L. Sulphate resistance and passivation ability of the mortar made from pozzolan cement with zeolite. *J Therm Anal Calorim*. 2008;94:7–14.

3. Sersale R. Structure et caractérisation des pouzzolanes et des cendres volantes. Proceedings of the 7th international congress on the chemistry of cement, vol IV-1. Paris; 1980. p. 3–21.
4. Chan SYN, Ji X. Comparative study of the initial surface absorption and chloride diffusion of high performance zeolite, silica fume and PFA concretes. *Cem Concr Compos.* 1999;21: 293–300.
5. Poon CS, Lam L, Kou SC, Lin ZS. A study on the hydration rate of natural zeolite blended cement pastes. *Constr Build Mater.* 1999;13:427–32.
6. Gayoso Blanco RA, Lam MR. Non-conventional aggregates and mineral admixtures in high-performance concrete. *ACI Special Publ.* 2003;228:123–34.
7. Mertens G, Snellings R, Van Balen K, Bicer-Simsir B, Verlooy P, Elsen J. Pozzolanic reactions of common natural zeolites with lime and parameters affecting their reactivity. *Cem Concr Res.* 2009;39:233–40.
8. Snellings R, Mertens G, Hertsens S, Elsen J. The zeolite-lime pozzolanic reaction: reaction kinetics and products by in situ synchrotron X-ray powder diffraction. *Microporous Mesoporous Mater.* 2009. doi: [10.1016/j.micromeso.2009.05.017](https://doi.org/10.1016/j.micromeso.2009.05.017).
9. Luke K. The effect of natural zeolites on the composition of cement pore fluids at early ages. Proceedings of the 11th international congress on the chemistry of cement. Montreal; 2008. unpage.
10. Taylor HFW. Cement chemistry. London: Academic Press; 1999.
11. Roszczynialski W. Determination of pozzolanic activity of materials by thermal analysis. *J Therm Anal Calorim.* 2002;70: 387–92.
12. Dweck J, Cherem da Cunha AL, Afonso Pinto C, Pereira Gonçalves J, Büchler PM. Thermogravimetry on calcined mass basis-hydrated cement phases and pozzolanic activity quantitative analysis. *J Therm Anal Calorim.* 2009. doi: [10.1007/s10973-008-9761-0](https://doi.org/10.1007/s10973-008-9761-0).
13. Vessalas K, Thomas PS, Ray AS, Guerbois J-P, Joyce P, Haggman J. Pozzolanic reactivity of the supplementary cementitious material pitchstone fines by thermogravimetric analysis. *J Therm Anal Calorim.* 2009. doi: [10.1007/s10973-008-9708-5](https://doi.org/10.1007/s10973-008-9708-5).
14. Wu ZQ, Young JF. The hydration of tricalcium silicate in the presence of colloidal silica. *J Mater Sci.* 1984;19:3477–86.
15. Gartner EM, Young JF, Damidot DA, Jawed I. Hydration of Portland cement. In: Bensted J, Barnes P, editors. Structure and performance of cements. 2nd ed. London: Spon Press; 2002. p. 57–113.
16. De Silva PS, Glasser FP. Hydration of cements based on metakaolin: thermochemistry. *Adv Cem Res.* 1990;3:167–77.
17. Alonso S, Palomo A. Calorimetric study of calcium hydroxide-metakaolin solid mixtures. *Cem Concr Res.* 2001;31:25–30.
18. Mostafa NY, Brown PW. Heat of hydration of high reactive pozzolans in blended cements: Isothermal conduction calorimetry. *Thermochim Acta.* 2005;435:162–7.
19. Sanchez de Rojas MI, Frias M. The pozzolanic activity of different materials, its influence on the hydration heat in mortars. *Cem Concr Res.* 1996;26:203–13.
20. Garcia de Lomas M, Sanchez de Rojas MI, Frias M. Pozzolanic reaction of a spent fluid catalytic cracking catalyst in FCC-cement mortars. *J Therm Anal Calorim.* 2007;90:443–7.
21. Gutmann V. The donor–acceptor approach to molecular interactions. New York: Plenum Press; 1978.
22. Yamamoto S, Sugiyama S, Matsuoka O, Kohmura K, Tadatoshi H, Yasuyuki B, et al. Dissolution of zeolite in acidic and alkaline aqueous conditions as revealed by AFM Imaging. *J Phys Chem.* 1996;100:18474–82.
23. Ragnarsdottir KV. Dissolution kinetics of heulandite at pH 2–12 and 25 °C. *Geochim Cosmochim Acta.* 1993;57:2439–49.
24. Bish DL, Carey JW. Thermal properties of natural zeolites. In: Bish DL, Ming DW, editors. Natural zeolites: occurrence, properties, applications. Reviews in Mineralogy and Geochemistry 45. Washington, DC: Mineralogical society of America; 2001. p. 403–52.
25. Double DD, Hellawall A, Perry SJ. The hydration of Portland cement. *Proc R Soc Lond.* 1978;359:435–51.
26. Liebau F. Structural chemistry of silicates: structure, bonding, and classification. Berlin: Springer-Verlag; 1985.